Suez Canal Engineering Energy and Environmental Science Journal
Faculty of Engineering – Suez Canal University

2025, Vol. 3, NO. 1, Pages 26-42

Analysis on Different Decoupling Methods for MIMO Antenna in Ultra-Wide Band Applications: A Review

Aya A. Emam[1*], Osama M. ElGhandour[2], Eyad S. Oda[1], Ahmed E. Magdy[1]

[1] Electrical Department, Faculty of Engineering, Suez Canal University, Ismailia, Egypt
[2] Communication Department, Faculty of Engineering, Helwan University, City, Egypt

**Corresponding author: Aya A. Emam, Email address: ayaemam226@gmail.com*
DOI: 10.21608/SCEEE.2024.329148.1046,

Article Info:
Article History:
Received: 17\10\2024
Accepted: 08\12\2024
Published: 30\01\2025

DOI: 10.21608/SCEEE.2024.329148.1046

Abstract

Multiple-input multiple-output (MIMO) Ultra-Wide Band are a popular study topic in wireless communication technology as it can enhance the channel capacity of the antenna system to meet new communication needs while maintaining bandwidth and transmission power. However, increasing the number of antenna elements in a given space can result in mutual coupling effects, reducing transmission quality. As a result, it is critical to build a small MIMO wireless system using decoupling techniques. Several studies to reduce mutual coupling effects have been proposed. However, an extensive review of the characteristics and similarities amongst various decoupling methods is missing. This paper provides a comprehensive review of studies on the mutual coupling effect in MIMO. Then, several decoupling approaches that are important are classified, discussed and full examination of the benefits and drawbacks of each decoupling strategy. The article summarizes the impact of various decoupling designs and discusses their potential usability and flaws.

Keywords: *MIMO, UWB, Mutual Coupling*

Suez Canal Engineering, Energy and Environmental Science Journal (2025), Vol. 3, No.1.

1. Introduction

Ultra-wideband (UWB) antennas play a crucial role in wireless communication networks, prompting significant research interest. Recent research has focused on UWB communication technologies to meet the demand for high data speed, low cost, and low power (Lim et al., n.d.). Planar antennas are becoming more popular for UWB applications since the Federal Communications Commission (FCC) assigns UWB an unlicensed frequency range of 3.1 GHz to 10.6 GHz (S. M. Abbas et al., 2018). Microstrip type antennas is commonly employed in UWB wireless applications because to its ease of implementation, good frequency response, and compatibility with other equipment (Awan et al., 2021). UWB antennas are commonly used for radar systems, X-band (Suresh et al., 2022), public security, Ku- band. UWB antennas have smart applications such as vehicle radar systems, surveillance systems, software-defined radios, spectrum analysis, and proximity fuses (Suresh et al., 2022). Research challenges in UWB antennas include wide impedance matching, radiation stability, low profile, small size suitable cost, and a multipath fading (Alharbi et al., 2022).

To prevent signal fading from multipath effects, diversity systems with two receivers have been developed, which was the beginning of the evolution of MIMO (Beverage, n.d.,1931),(Peterson, n.d.,1931). Existing research (Jensen, 2016),(Sengar, 2014) has demonstrated that, as compared to single input single output (SISO) systems with a simple structure, MIMO systems have more additional paths, and the multipath effect, delay, and packet loss can be minimized to improve communication modes. Furthermore, Shannon's theorem states that channel capacity is proportional to channel bandwidth and signal-to-noise ratio.

In this research, we study decoupling methods for MIMO systems. We demonstrated some good MIMO decoupling techniques over the last five years and analyzed the potential challenges they face. These methods are classified into two types: external decoupling techniques and internal decoupling techniques. External decoupling approaches use additional structures to counteract mutual coupling, which are further classed as neutralization lines (NL), parasitic decoupling elements (PDE), defective ground structures (DGS), metamaterial techniques, and so on. Internal decoupling approaches are related to orthogonal and multi polarization being the most widely utilized.

The remainder of this paper is organized as follows, the second section focusses on the reasons for mutual coupling and its negative impact on MIMO systems. The third section explores different decoupling methods in MIMO wireless networks that are applicable to UWB. Section four provides a full examination of the benefits and drawbacks of each decoupling strategy, also discusses the future direction of decoupling methods. In the final section this survey has concluded.

2. Mutual Coupling Issue

The information theoretical capacity in MIMO systems increases linearly with the number of elements (Foschini, 1998). Later, Wallace and Jensen (Wallace, 2004) pointed out that the linear rise in channel capacity was not unconditional, and it was accomplished by arranging antenna elements with broad separation (more than several wavelengths). However, this is difficult for present mobile customers as most 5G applications, particularly portable devices, are made up of integrated circuits with antenna elements separated by only one wavelength. In this short space, the electromagnetic interference between antenna elements is known as the mutual coupling effect, which makes issue in MIMO systems.

2.1. Mutual Coupling Reasons

When studying the reasons for mutual coupling, the focus is on analyzing the effect of current. The working basis of antennas, regardless of their shape, is based on the same method of radiation generated by changing speed charges (Balanis, 1992). In MIMO systems, mutual coupling effects can be caused by three different factors.

1)- Near field coupling. When the antennas are close together, they are in the same field zone as other antennas. And The effect of near-field electromagnetic waves is dominant (Nikolic, 2005). According to (C. ; L. E. ; S. D. F. Wang, 2017), the decay of this field follows a distance of ρ^{-2} or ρ^{-3}.

2)- Surface-wave coupling. This coupling often occurs in microstrip antennas, due to sharing the same ground plane (Chen, 2018). During the feeding process of the antenna element at the feed point, a distributed current is generated on the ground plane. This current will flow to nearby antenna elements, dispersing the energy and creating interference.

3)- Free-space coupling. When an excitation element generates electromagnetic waves, some of the energy is absorbed by surrounding antennas, leading them to generate additional currents. Surface waves contribute less to mutual coupling than space waves due to their slower fading at $\rho^{-1/2}$ compared to ρ^{-1}(Khayat, 2000).

2.2. Negative Effects of Mutual Coupling

Mutual coupling has both positive and negative effects on MIMO systems. The negative impacts are the topic of this paper. First, mutual coupling has major impacts on the average bit error ratio (BER) of MIMO systems, particularly at antenna element separations of 0.3-0.5 wavelength, Figure 1 the BER at two different distances between the antennas, A spacing of 0.5λ (low coupling) has a negligible impact on BER as in Figure 1.(a) , 0.1λ element spacing(high coupling), the results indicate that BER is higher in case of high coupling, low correlation as in Figure 1.(b) (Abouda et al., n.d.,2006)

.

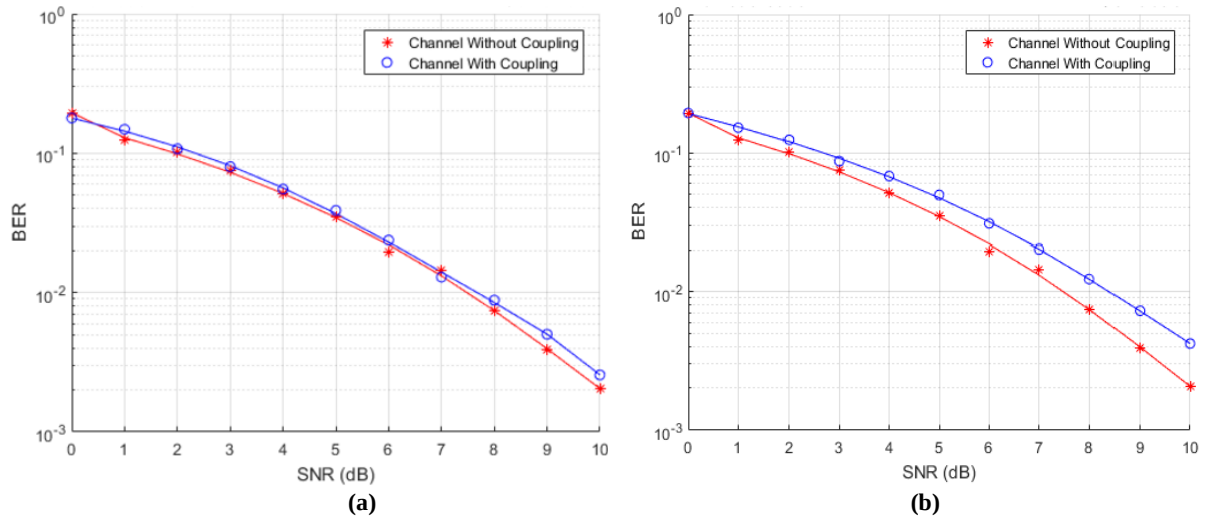

(a) **(b)**

Figure 1. BER at different distances between antenna elements (a) at 0.5λ, (b) at 0.1λ.

Furthermore, in terms of radiation pattern (Lee, 2021), a distortion of radiation pattern occurs in MIMO antennas when compared to the isolated radiation pattern of each element as in(Emam et al., 2024) the authors designed a novel design for

MIMO systems, Figure. 2 shows radiation patterns at 10.4 GHz for the MIMO antennas with and without the decoupling, the comparison highlights some of the distortion in the coupled antennas, clearly demonstrating the impact of mutual coupling on the system performance.

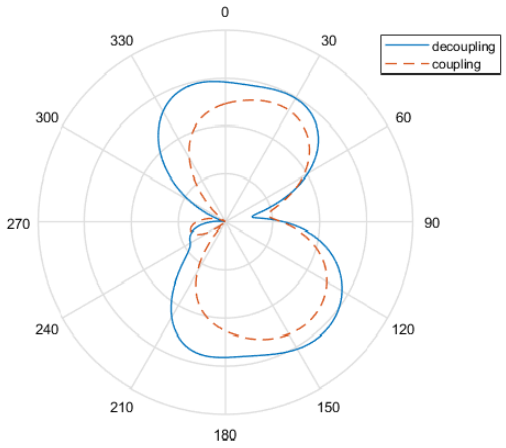

Figure 2. Example of radiation pattern with and without decoupling

The accuracy of estimating direction-of-arrival (DOA) in MIMO systems may decrease significantly at high frequencies due to mutual coupling in the array manifold (Weiss, 1988). Finally, if the endpoint contains several coupling receivers, the large capacity of MIMO can be evaluated using bias (Janaswamy, 2002). Mutual coupling reduces received signal-to-noise ratio (SNR) at receiver spacings between 0.35-0.5 wavelengths, resulting in lower channel capacity than intended.

To summarize, mutual coupling affects MIMO systems through two aspects. As For The output terminals generate the desired EM field using currents with a specific frequency. EM fields generated by currents and neighboring antennas can easily affect transmitting antennas due to their close distance. Combining multiple electromagnetic fields changes the phase and amplitude of the original current. As for input terminals, when the input signals are transmitted to the receiving port, the current is not only induced, but also radiated again. As a result, the essence of the signal collected at the receiving port is the vector sum of the EM wave produced by the output terminals and re-radiated fields. We can see that it is essential to reduce the negative impacts of mutual coupling in MIMO systems.

3. Decoupling Methods:

In recent years, various decoupling solutions have been presented to meet isolation requirements or increase channel capacity in MIMO systems. These techniques can be classified as external or internal as in Figure 3, based on the decupling methods.

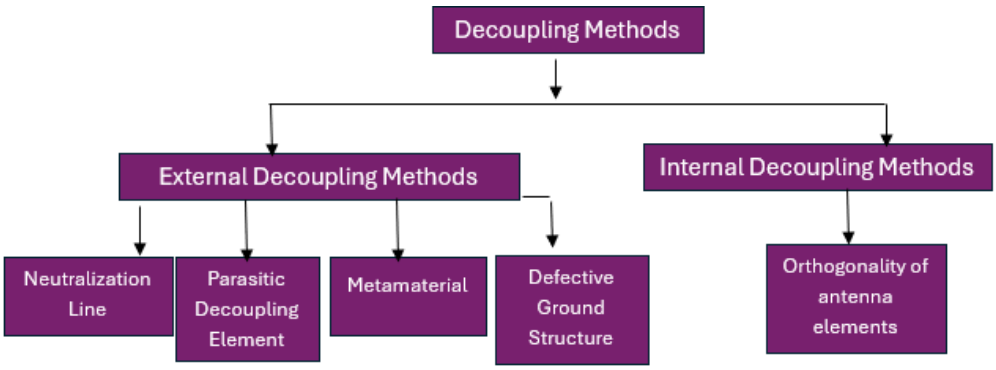

Figure 3. Mutual Coupling Methods

3.1. External Decoupling

External decoupling requires placing structures between nearby antenna elements. Two categories can be defined based on various mutual coupling suppression techniques. Neutralization lines (NL) and parasitic decoupling elements (PGE) are examples of new coupling paths that offset the current one. Other methods for controlling or reducing surface current flow include defective ground structures (DGS), metamaterials approaches, and so on.

3.1.1. Neutralization Line:

This Decoupling Technique improves isolation by attaching NL to both antenna elements. This creates the additional current path between the MIMO antenna's two antenna elements. Its main benefits include cost-effectiveness and simplicity, making it easy to integrate into current antenna designs without taking up much room. Furthermore, NLs provide

comprehensive efficacy at a variety of frequencies. Optimizing its design can be complicated and may not significantly enhance additional performance metrics, including radiation patterns. NLs are an important tool in current antenna design, with typical applications including MIMO antenna arrays, wireless communication devices, miniature antennas for wearables, and triband systems.

As shown in Figure 4. (a)s, the antenna element was designed in reference (Tiwari et al., 2019)by combining a modified rectangular patch with a semi-circular patch. The NL was coupled with two antennas to increase the isolation between the two ports. This work (Masoodi et al., 2022)The antenna is made up of RT Rogers 5880 substrates with defective ground structure on the back and T over T shaped meander microstrip lines printed on the front that can generate a resonance mode. An I-shaped ground slot improves isolation in the case of a two-element MIMO antenna. The 10 mm neutralization line (NL) at both hands facilitates the mutual coupling reduction as shown in Figure 4. (b).in (Ma et al., 2023) A four-port L-type MIMO antenna that can operate at 4.4–4.9 GHz, 5.4–6.1 GHz, and 7.0–7.4 GHz is suggested. It does this by using the decoupling techniques of T-branch, defective ground structure, and neutralization-line as shown in Figure 4. (c). The neutralization lines are intended to create a 180 ° phase shift at 4.5 GHz and 5.7 GHz, thereby canceling out the coupling current from port 1 to port 3(|S31 |). This antenna provides isolation of more than 20 dB. Consequently, at 4.5 GHz and 5.7 GHz, respectively, |S31 decreased by 13 dB and 15 dB.

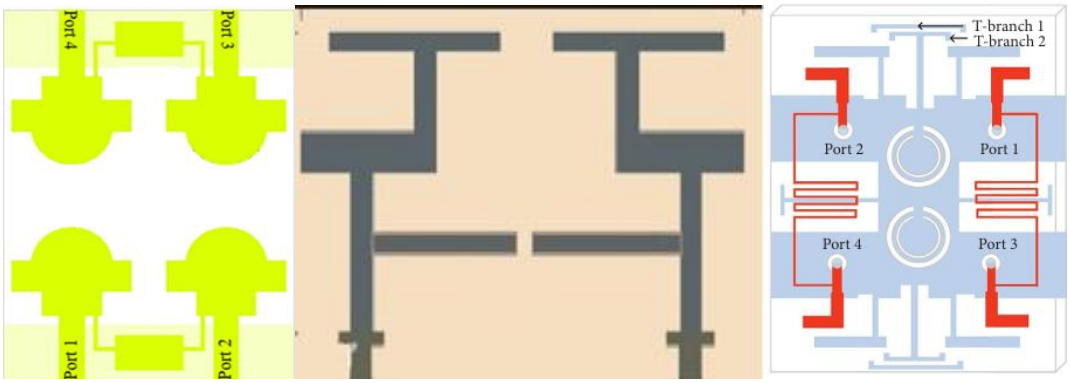

(a) **(b)** **(c)**

Figure 4. MIMO antenna with neutralization line, (a) (Tiwari et al., 2019), (b) (Masoodi et al., 2022) and(c) (Ma et al., 2023)

In(Dkiouak et al., 2023)the antenna is made up of two symmetrical radiators positioned next to each other on a FR-4 substrate. To obtain more than 16.5 dB of isolation between the antenna elements throughout the UWB, a vertical T-shaped neutralization line is introduced into the ground plane. The purpose of inserting this metallic wire is to offset the electromagnetic field that is present in the proposed structure at the UWB. This approach enhances the antenna's isolation between its radiators, which enhances other properties of the MIMO UWB antenna.

A novel neutralization-line-incorporated decoupling network (NLDN) for wideband multielement antenna arrays is proposed in this (Zou et al., 2023). Based on network model derivation and node analysis, the wideband antenna arrays are well matched and isolated through the introduction of additional current path supplied by neutralization line (NL) between antenna elements and decoupling network (DN) between feeding lines, but without extra matching network to counteract with the original path in (Munusami & Venkatesan, 2024) a compact boat-shaped dual-band MIMO antennas improve separation for 5G and WLAN applications. To reduce mutual coupling by -21 dB at 2.32 GHz and -44 dB at 5.2 GHz, a ladder-shaped slot decoupling structure is first installed in the ground plane. To improve the isolation, neutralization lines (NL) are also connected to the two radiating elements above the substrate. The diagonal arrangement of the radiating parts causes the current flow's phases to be opposite of one another. The current flow is cancelled when the neutralization lines are introduced because they create an extra coupling path against the radiating elements. The MIMO antenna in (Z. Wang et al., 2022)is composed of up of two radiating patches, a semicircle and a semi-regular hexagon in each, in addition to surface-etched C and U slots that adjust the antenna's characteristics for return loss. On the other hand, a neutralization line is generated, which restricts the amount of current that may be transmitted on the ground plane. To enhance the isolation between the radiation elements, a cross-shaped slit is also used in the center of the ground.

In (John et al., 2024)compact, flexible, four-element MIMO antenna designed for wearables operating at sub-6 GHz. A unique hybrid decoupling structure that suppresses the coupling current and offers isolation greater than -24 dB across the bandwidth is made possible by a neutralization line in the radiator and a unique defective ground structure (DGS). By keeping the antenna's reflection coefficient constant, a special DGS has increased isolation. The increase of bandwidth is allowed by the rectangular slots located in the ground of each individual element.

3.1.2. Parasitic Decoupling Elements

Parasitic elements are carefully placed in MIMO systems to enhance antenna performance, including gain, directivity, and impedance matching. It increases the impedance bandwidth by using coupling mechanisms in the ground plane or radiation patch.

The design is basic and may be simply suited into existing structures, without any requirement of additional space Additionally, it works well across a wide frequency range. However, adjusting the size and positioning of parasitic elements

can be difficult, and it may not significantly improve other performance parameters, like as gain or radiation patterns, despite improved isolation. This technology is widely utilized in slot antennas and wireless communication devices, MIMO antenna arrays, and small wearable designs, emphasizing its significance in contemporary antenna engineering.

The authors (sim, Devana, Islam and Godi) show recent improvements in the design of a dual-port MIMO antenna that can operate across several frequencies. The dual-band MIMO antenna with minimal mutual coupling suggested in Ref. (Sim et al., 2023) The identical monopole radiators use a rectangular patch, inverted-E, and asymmetrical T-shaped strip to generate 5G Sub-6 GHz and Wi-Fi 6E frequencies. A parasitic dollar-shaped structure (PDSS) is inserted between the two monopole radiators to suppress the surface waves of each monopole, reducing the measured mutual coupling by up to -15 dB over the working band. effectively isolates 5G millimeter-wave networks, with a maximum gain of 2.65 dBi and isolation of 15 dB. Ref. (Devana et al., 2024) describes a compact MIMO UWB antenna with a peak gain of more than 4.93 dBi for 5G Antenna-in-Package Design at Millimeter-Wave Frequencies. The MIMO antenna uses octagonal radiators made from tapered microstrip line-fed rectangular patches. Parasitic stubs are strategically exploited to minimize coupling among MIMO elements, as shown in Figure 5. (a), the isolation level is less than 20 dB. According to (Islam et al., 2024), a UWB MIMO antenna with two elements operates between 2.3-17.8 GHz and achieves a gain of over 6.5 dBi. A meandering line shaped as in Figure 5. (b) is added to minimize the mutual coupling between closely spaced MIMO elements to less than 25 dB. (Pradeep et al., 2024)An UWB MIMO antenna with two elements operates between 3.6-7 GHz and has a gain of more than 6.5 dBi. The design considers the slot's impact on both the ground plane and the parasitic strip line to increase performance, isolation, and impedance matching among antennas. In(Godi et al., 2024) to reduce the effect of coupling, a rectangular parasitic decoupler is positioned between the two elements. The results show that the antenna resonates at 6 GHz, and coupling is reduced by 14 dB employing a parasitic decoupler. S12 and S21 produced with a parasitic decoupler are the same at 33.06 dB.

In (Zeain et al., 2024)this research presents a novel Chair-shaped MIMO antenna with two radiating elements and a single layer of frequency-selective surface (FSS) for 5G Sub-6GHz communication systems. They employ two methods for isolation and gain enhancement: parasitic elements and (FSS) The 1 × 2 MIMO antenna feeds from a coplanar waveguide (CPW). Furthermore, an FSS array structure consisting of (a 68-unit) Square-shaped structure with Circular Slot (SCS) shaped cells is used, along with a new approach (Surround approach), to improve the gain and isolation between the MIMO antenna elements. In (Elabd & Al-Gburi, 2023), Elabd and Ahmed developed a two-element MIMO antenna array for MM Wave 5G mobile devices, encompassing the 28/38 GHz frequency ranges. This antenna array, which employs dual-mode planar dipole antennas, has significantly improved isolation and gain. To enhance ECC and isolation between MIMO antenna elements, the element spacing, including the parasitic element is precisely set at 0.5λ₀. Furthermore, improvements are found in TARC, EG, and DG.

Academic research has mostly concentrated on improving four-port MIMO antennas, as the author shows (Esmail and Abbas). In (Esmail et al., 2024), MIMO antenna for 5G millimeter-wave indoor applications is described. Each element is composed of two connecting patches. The primary patch is connected to the inset feed, and the secondary patch is arc-shaped and placed over the main patch, opposite the feed. The MIMO antenna has a gain that exceeds 7 dBi at both frequencies. An array of four antennas is set orthogonally to form a MIMO system with isolation greater than 19 dB. The isolation is further enhanced by the placement of a circular parasitic patch at the front and changes made to the ground. According to (A. Abbas et al., 2023), each single-element antenna has a radiating patch, substrate, ground plane, electromagnetic bandgap (EBG) structures, and split ring resonators (SRR). To achieve the desired UWB bandwidth, the antenna patch's lower edges are cut with a quarter-circle radius. A unique parasitic decoupling structure reduces the excessive isolation between elements. The decoupling structure is designed to eliminate mutual coupling in all passbands.

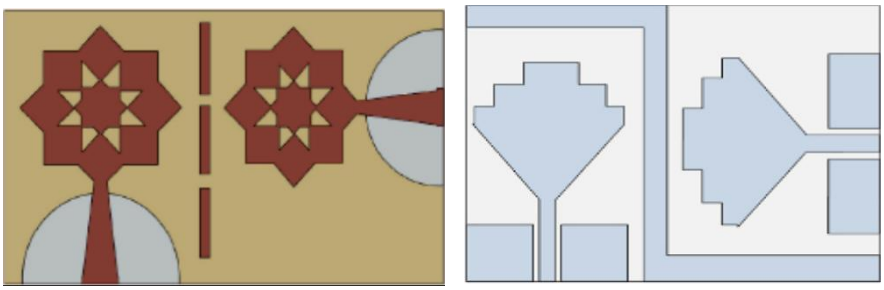

(a) **(b)**

Figure 5. MIMO antenna with PDE, (a) (Devana et al., 2024), (b) (Islam et al., 2024).

3.1.3. Metamaterial:

A. Electromagnetic Band Gab (EBG)

In the area of antenna engineering, EBG structures have an important role for reducing surface waves and improving antenna performance. Periodic structures known as Electromagnetic Band Gap (EBG) structures have a band gap that blocks electromagnetic radiation from propagating within a certain frequency range. To minimize surface waves, using EBG as ground planes or reflectors might increase their effectiveness and gain. To achieve ideal performance, the EBG unit cell characteristics and the spacing between the antenna and EBG must be properly designed. EBGs allow antennas to

be placed closer to the ground plane, leading in more compact designs. However, designing EBGs with practical capacity at lower microwave frequencies and achieving broad performance continues to be effective. Electromagnetic Bandgap (EBG) structures provide high isolation levels, often exceeding 25 dB, which is an advantage. This capability prevents interference while improving overall performance. Furthermore, EBG structures can improve radiation patterns and customize in size and shape to specific applications, making them ideal for compact devices like smartphones and IoT items. Designing good EBG structures can be time-consuming and complex, with the potential for increased losses and bandwidth limits. EBG is particularly useful in MIMO systems, wireless communication devices, medical imaging, and satellite communication, where strong isolation and dependable performance are required.

The antenna elements in reference to (Jabire et al., 2021) have been constructed out of a partial ground with stubs and modified circular radiators fed by microstrips. To increase bandwidth and reduce mutual coupling, a metamaterial structure was placed around the feed line on both sides as shown in Figure 6. (a). As shown in Figure 6. (b),(Kulkarni et al., 2021) reference by placing a "EL" slot into the radiating element and coupled two identical stubs to the partial ground to enhance impedance matching and radiation characteristics across the band. An un-protruded multi-slot (UPMS) isolating element was positioned between two closely spaced ports to achieve high port isolation as shown in Figure 6. (b). In (A. Khan et al., 2021)Two radiating patches share a partial ground plane. The designed antenna has minimal mutual coupling because of a ground stub and a single column Electromagnetic Bandgap (EBG) construction between the two radiating patches. The mutual coupling is reduced with the addition of a ground stub. When an EBG column is added between the two radiating elements, there is an additional decrease in mutual coupling as shown in Figure 6. (c). In (Tan et al., 2022)there are two carefully placed mirror-symmetric dual-branch antennas. An M-EBG structure for greatly minimizing mutual coupling between two tightly packed dual-branch antenna arrays has been provided by this design. At the resonant frequency, the isolation has improved by 31.9 dB when compared to the reference antenna.

In (N. Kumar et al., 2023) two closely spaced multiband antenna elements are placed in the E-plane. The single MIMO antenna element has a modified ground structure, a U-shaped radiating patch with a slot is designed to operate as a triple band antenna on a FR4 substrate. For the frequency bands 5.38~5.73 GHz, 6.22~8.88 GHz, and 9.56~11.8 GHz, simulated mutual coupling is reduced after applying the EBG structure, with a greatest reduction at 5.53 GHz, 6.9 GHz, and10.77, respectively. In(Tamminaina & Manikonda, 2023) This design presents a compact, four port MIMO antenna with a G slot for supporting 5G communication. This antenna contains an S-shaped (EBG) formed on the substrate between two adjacent radiating patch pairs. At 3.6 GHz, the isolation of a four-port G-slot MIMO antenna with an S-shaped EBG structure is enhanced by 10 dB, and the mutual coupling between the antennas is reduced as the S12 value falls to ~-38 dB. This illustrates how a four port MIMO antenna constructed with an EBG provides better port isolation. In(Li et al., 2024) to improve isolation and bandwidth in a compact UWB-MIMO antenna, a novel stepped EBG formed on the T-shaped stepped stub is described. It works in combination with an inverted H-shaped slot etched on the ground. The combined approach of the lower and higher EBGs to construct a stepped EBG is utilized. The MIMO achieves better behavior than higher EBG only or lower EBG only because it has a better impedance bandwidth and isolation larger than -20 dB. The step EBG provides an improvement in isolation and impedance bandwidth in the lower range of the operating band when compared to the higher ones.

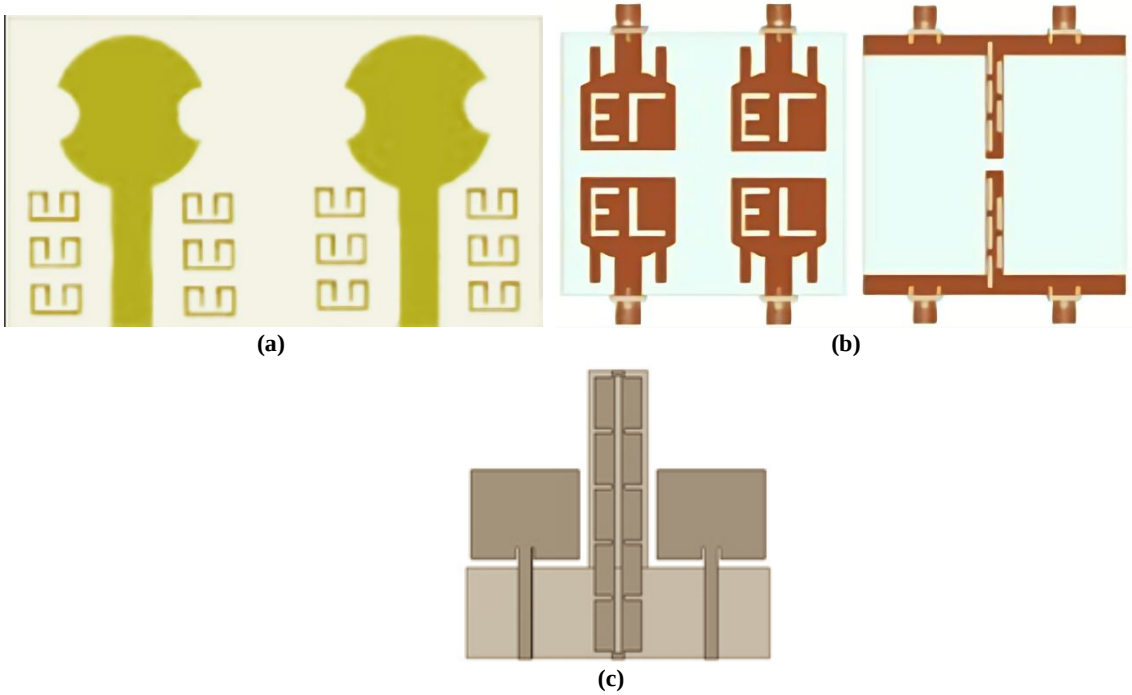

(a) **(b)**

(c)

Figure 6. MIMO antenna with EBG (a) to (Jabire et al., 2021),(b) (Kulkarni et al., 2021),(c) In (A. Khan et al., 2021)

In (Babu et al., 2023)for ultrawideband (UWB) systems, a two-port disc-shaped multiple-input multiple-output (MIMO) antenna is studied. The construction of the MIMO antenna with EBG. The antenna is constructed from a ground surface on the back of the substrate and two identical disc-shaped monopole elements placed parallel on the upper facet of the substrate. The decoupling structure between the MIMO antenna elements is an EBG array. It increases isolation to 22 dB and impedance bandwidth to 120%. The design of a compact, two-element, ultra-wideband (UWB) electromagnetic band gap (EBG) multiple-input multiple-output (MIMO) antenna with improved isolation is shown in this (Suresh Babu et al., 2023). The unit cell consists of a square-shaped radiator that is formed by connecting an elliptical element to a rectangular monopole, and to improve the isolation between the square-shaped radiator elements, a 1*4 sized EBG array is also included. The EBG array suppresses surface wave effects to increase coupling between identical radiating parts, improving isolation and impedance bandwidth. A fractional bandwidth of 114.9% (3.0–11.1 GHz), isolation of more than 24 dB, and peak gain of roughly 9.6 dBi above UWB are all achieved by the suggested square-like MIMO radiator with EBG. In (Saxena et al., 2021), a planar two-element super wideband MIMO antenna has been designed. In order to achieve high isolation (<-20dB) and high diversity performance in the super wideband range, a circular ring is etched on an elliptical patch of antenna and a complementary split ring resonator (CSRR) on the ground plane. Additionally, the EBG technique is deployed near the microstrip feed line, yielding an ECC less than 0. 0018.

B. Split Ring Resonators (SRR)

Split Ring Resonators (SRRs) play a crucial role in antenna engineering, allowing for feasible and compact antenna designs. They improve antenna performance by creating a resonant effect, allowing for more exact frequency calibration.

SRRs are commonly used in antenna designs due to their magnetic resonance features and unique interaction with electromagnetic radiation. Printed circuit board fabrication requires careful consideration of design characteristics such ring width, gap size, and substrate material. Using SRRs in space-constrained applications leads to antennas with enhanced multiband capabilities, better operational performance, and smaller footprint. This is a valuable quality. However, the resonance frequency may be sensitive to external conditions, and their design difficulties and fabrication techniques can be difficult (Nornikman et al., n.d.; Zhao et al., 2011).

SRRs offer high isolation between closely placed antennas, minimizing mutual coupling and increasing MIMO system efficiency. They may also be tuned to specific frequencies, allowing for customized performance across a variety of applications.

Additionally, while SRRs provide great isolation, their performance may be confined to specific frequency bands, limiting their usage in wideband applications. SRRs improve the quality of signals and reduce interference in wireless communication systems, resulting in better antenna performance.

Researchers have recently designed a two-element MIMO antenna that can operate across multiple frequencies authors (D. Khan and Sakli). In Ref. (D. Khan et al., 2024), the author presents a two-band 5G MIMO antenna that operates at 28 and 38 GHz, with a peak gain of 7.8 dB and 30 dB isolation as in Figure 7. (a). Reference (Sakli et al., 2021) as in Figure 7. (b)describes a two-element ultra-wideband (UWB) MIMO antenna optimized for performance and compactness by placing antennas closely together.

Research has focused on the usage of four-port MIMO antennas. Reference (Singh et al., 2023) describes a frequency reconfigurable multiband MIMO antenna for 5G communication systems with a maximum gain of 1.74 dB and isolation of more than 28 dB as in Figure 7. (c). Reference (Rajeshkumar & Rajkumar, 2021) describes a multiband MIMO antenna with four elements that exhibits additional resonance at 5.1 GHz and achieves an isolation level of 14 dB.

(a) **(b)**

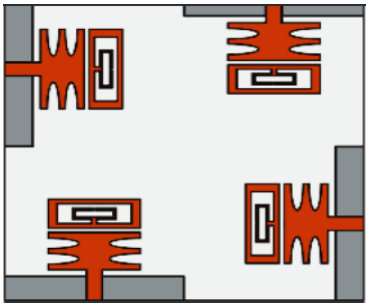

(c)

Figure 7. MIMO antenna with SRR (a) . (D. Khan et al., 2024),(b) (Sakli et al., 2021) and (c) (Singh et al., 2023)

Research has focused on the use of eight-port MIMO antennas. Reference. (A. Khan et al., 2023), the author describes an eight-element UWB MIMO antenna that has 20 dB isolation level and a maximum gain of 7 dBi. In Reference(Huang et al., 2023) , the author describes a compact eight-port MIMO antenna array for 5G sub-6 GHz handset applications working between 3.3-5 GHz, with a maximum gain of 3 dB and isolation of 12 dB.

Christina et al. (Christina et al., 2024) proposed a method to minimize MC between two tri-band antennas for LTE, WLAN, and 5G applications, which covers several stages. Initially, a monopole is optimized for functioning at 3.5 GHz, with modifications to the partial ground plane to produce resonance at the remaining two frequencies. This method produces a MIMO antenna system with two tri-band monopoles. Low-band resonators are specifically located to reduce mutual coupling in higher frequency bands through restricting surface wave propagation. A SRR reduces coupling even further in the low band. The resulting MIMO antenna supports WLAN, 5G, and LTE frequencies in the 2.4, 3.5, and 5.8 GHz bands. The maximum return loss values are 22 dB, 35 dB, and 38 dB, respectively, with mutual coupling levels of 25 dB, 18 dB, and 32 dB.

Zhang et al. (J. Zhang, 2020)investigated a wearable multi-antenna system that can withstand bending. Two conventional techniques for passive mutual coupling suppression, using electromagnetic bandgap structures and defective ground structures (DGS), are tested for their performance during bending or deformation. The development of a novel isolator inspired by metamaterials is critical for overcoming the constraints of traditional isolators in on-body applications. This unique design combines DGS with modified split ring resonators (SRR) to provide consistent isolation performance and extensive coverage, even under severe bending situations. Importantly, it retains the compact structure of a linear array. Using this isolator ensures a low envelope correlation coefficient between the two on-body antennas, which is crucial for increasing transmission efficiency in MIMO systems.

3.1.4. Decoupling Structure

The antenna in reference (Jetti & Nandanavanam, 2018) consisted of two identical rectangular radiators fed by CPW, as shown in Figure 8. (a.) A rectangular strip was placed to the ground surface to decrease mutual coupling and increase bandwidth. An inverted U-slot was added to the feed line in order to reject the WLAN spectrum. In (Mu et al., 2022) A radiating element in the shape of a flower was formed by combining three elliptically shaped metal patches that were spaced sixty degrees apart as shown in Figure 8. (b). The 4.3–15.63 GHz (relative bandwidth 113.4%) range is typically used for multi-standard wireless applications, such as 5G N79 (4.4–5 GHz), WLAN (5.15–5.35 GHz/5.72–5.825 GHz), 5G spectrum band (5.9–6.4 GHz), X-band for satellite communication (8–12 GHz), FSS (11.45–11.7 GHz/12.5–12.75 GHz), and Ku band (12–18 GHz). The adopted ground structure improvements comprise two modified inverted L-shaped branches and an I-shaped stub. By absorbing the current, these modifications also effectively reduce mutual coupling between the antennas, increasing isolation to over 20 dB.

In this study (Kempanna et al., 2023) provides a compact UWB MIMO antenna in the form of a vase. The isolation between the inter elements is improved by the special DGS decoupling structure. By placing a parasitic element on the ground plane that resembles an inverted pendulum, the UWB MIMO antenna's isolation is improved. In the 5–13.5 GHz operating frequency range, this modified ground plane serves as a decoupling structure and offers isolation below 21 dB. A compact two-port MIMO antenna in (Srinubabu & Venkata Rajasekhar, 2024) that has been designed to operate in the N78/48 band for 5G-NR FR-1 applications, A MIMO antenna with closely spaced elements just 1.5 mm, or 0.012 λ is included in the design. To improve isolation, the microstrip inserts a feeding line with a partially truncated ground, a grounded stub, and side stubs implanted in the ground plane. As in Figure 8. (c) T-shaped decoupling components are positioned between radiators to increase the antenna's bandwidth and enhance isolation (S21) over the band.

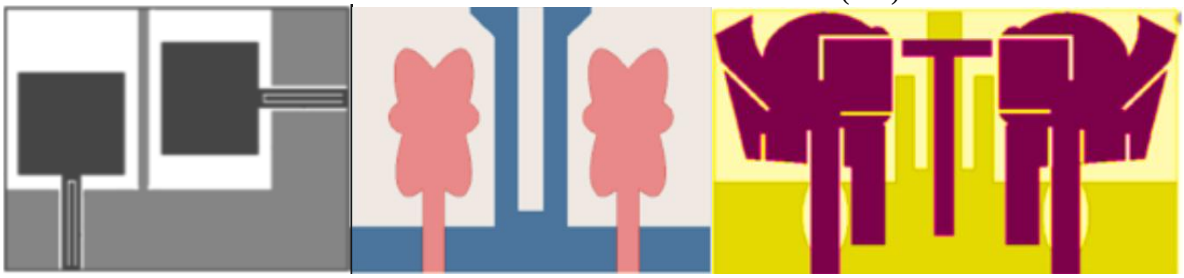

(a) **(b)** **(c)**

Figure 8. 2 port MIMO antenna with DGS (a) (Jetti, 2018),(b) (Mu et al., 2022) and (c) (Srinubabu & Venkata Rajasekhar, 2024)

Four identical rhombic-shaped monopole radiators placed orthogonally constructed the structure of the MIMO antenna described in reference (S. Kumar et al., 2020b), shown in Figure 9. (a). The antenna radiators were loaded with elliptical CSRR structures to block WLAN and Wi-MAX bands from the UWB spectrum, and a plus-shaped DS was added to provide good isolation.

The MIMO antenna in (S. Kumar et al., 2020a) was constructed up of four antenna elements, each of which had a square-slotted ground plane and a microstrip feed line. As shown in Figure 9. (b), a circular stub protruded from the ground plane

strip to accomplish circular polarization. Additionally, a rectangular strip was incorporated into the antenna's ground surface to provide high levels of antenna port isolation.

The MIMO antenna in (Jayant & Srivastava, 2023) included four monopole antenna elements with rectangular radiators that were fed by an L-shaped microstrip line. By using a cross-shaped DS and antenna elements oriented orthogonally, excellent isolation was achieved. By cutting two C-shaped slits from each radiator and adding an L-shaped slit in the ground for Wi-MAX NB, the developed antenna may implement WLAN and X-band NBs.

The antenna in (Addepalli et al., 2021) consisted of a modified substrate geometry and was constructed up of a circular arc-shaped conducting element on top. By repeating the elements orthogonally, a plus-shaped structure was established, resulting in polarization, variety and isolation. An inverted L-shaped strip and a semi-elliptical slot covering the partially ground comprised the modified ground plane, which benefited the antenna in achieving an expansive bandwidth.

In this work (P. Kumar et al., 2022) the outcome design is employed by using a unique decoupling structure consisting of six symmetrical pyramidal form UWB antennas with defective ground structures dispersed with parasitic components. The coupling effect is reduced, and the uniform current flow is disrupted by the grounded branches and modified rectangular stubs on the ground plane, which create closed and open current distribution channels. The inter-element coupling is reduced by the special decoupling structure formed up of parasitic elements with a rectangular layout and DGS with grounded branches.

In this study (O. Khan et al., 2023)proposes a compact 4-port UWB MIMO antenna. The dielectric material is a low-profile FR-4 substrate with standard thickness of 1.6 mm and dimensions of 58 * 58 mm. The impedance bandwidth of this design is characterized as ranging from 2.8 to 12.1 GHz (124.1%). The unit cells construct a quad-port MIMO antenna system with each unit cell oriented orthogonally as in Figure 9. (c). With a whirligig structure connecting the ground plane, this design provides significant isolation below 15 dB in the lower frequency range and below 20 dB in the higher frequency range. As a result, the port becomes less isolated at low frequencies. To improve the port isolation and impedance bandwidth even, symmetrically placed cross hook-shaped strips are added between the MIMO antenna elements.

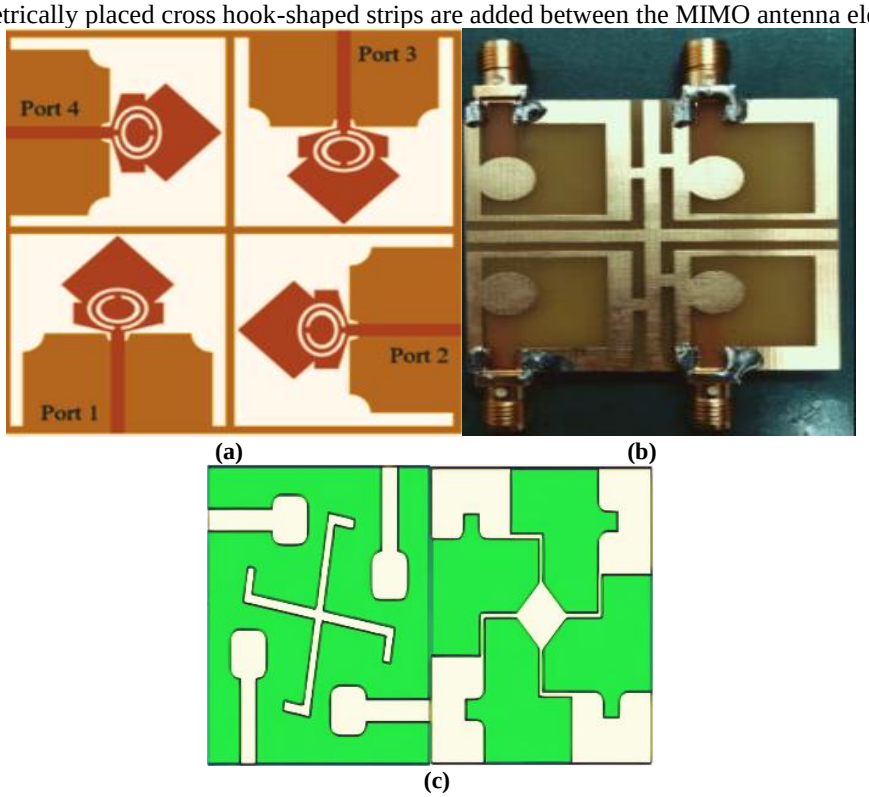

Figure 9. 4 port MIMO antenna with DGS (a) (S. Kumar et al., 2020b),(b) (S. Kumar et al., 2020a) and (c) (O. Khan et al., 2023)

3.2. Internal Decoupling (placing antenna elements in orthogonality)

In (Sultan & Abdullah, 2019) the antenna element, referred to as the quasi-self-complementary (QSC) strategy, was constructed of a half-elliptical monopole patch on the upper side and a corresponding half-elliptical slot added to the ground surface, as shown in Figure 10. (a). To achieve a wide bandwidth, a tapered transmission line stimulated the antenna. The orthogonal arrangement of the AEs improved isolation in the four-port MIMO configuration. The WLAN band was suppressed by adding a C-slot to the semi-elliptical radiator. As shown in Figure 10. (b), the antenna in paper (Naktong & Ruengwaree, 2020)was designed using stepped etching on the ground plane and an arrow-shaped slot placed on the radiating patch to increase bandwidth. The techniques of angular variation and homogeneous elements were utilized to

reduce mutual coupling between antenna elements. As shown in Figure 10. (c), in(Arumugam et al., 2021) the antenna element was constructed using modified elliptical radiators. With four elements placed orthogonally in a single plane, the antenna element further evolved into a MIMO antenna design. In paper (Govindan et al., 2022), the MIMO antenna consisted of four octagonal-shaped radiators with multiple slots loaded into them and placed orthogonally. The antenna elements in (Jayant et al., 2022) was a circular patch which offers improved impedance matching across the UWB range without the need for a feeding line. To form the MIMO antenna, the four antenna elements were placed across the four edges of a shared square-shaped ground. A four-port MIMO antenna with high isolation is illustrated in (Pandya et al., 2024). When vertical and horizontal conductive strips are appropriately included, a single antenna may achieve size compactness. Furthermore, the patch geometry is pooled and formed with a diagonal radiating strip. Receiving a wide band response and good isolation, respectively depends critically on the partial ground plane and the antenna elements placed orthogonally. The optimum isolation of 20 dB has been received.

For ultra-wide band applications, a quad-element MIMO antenna is proposed in this (Bsrat et al., 2022). By adding slots to the patch and defective ground constructing, the simple monopole antenna can be kept more compact and perform better. The results of the simulation compare various placements (orientations) for both two- and four-element MIMOs. It has been found that the quad-element MIMO antenna placed orthogonally performs better in terms of diversity and element isolation when operating in the UWB band. A quasi-elliptical self-complementary antenna provided by a coplanar waveguide (CPW) that shows super wideband characteristics and dual-band notches was presented in(Raheja et al., 2020) . The MIMO antenna's four radiating components were positioned orthogonally to one another to improve inter-element isolation and polarization variety. Every element in MIMO antenna had a slot that was a complement of a comparable shape and an elliptical-shaped conductor patch that were both located on the same side of the substrate.

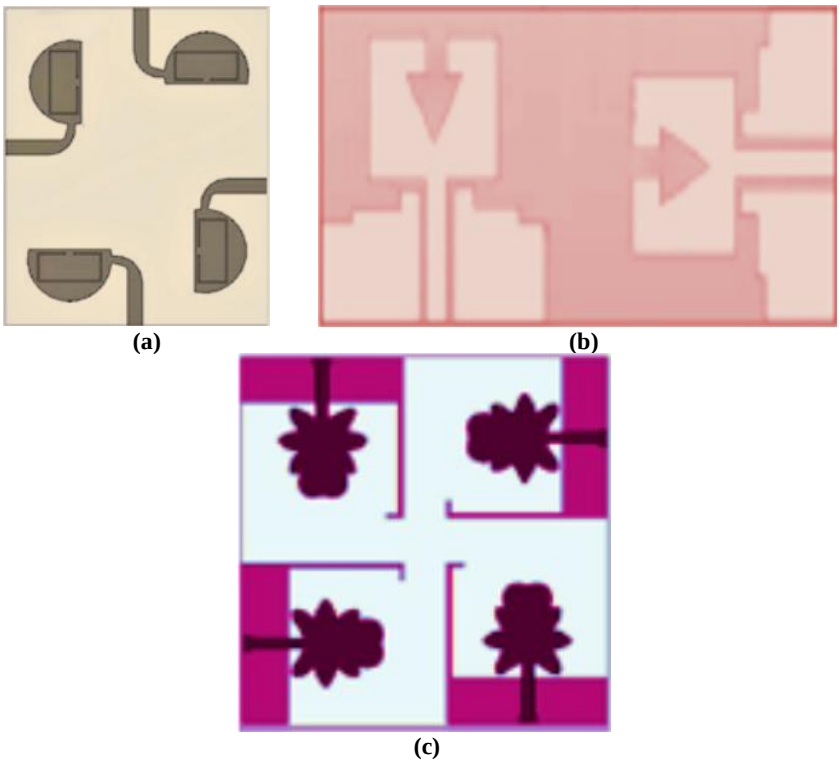

(a) **(b)**

(c)

Figure 10. MIMO antenna with orthogonal polarization, (a) (Sultan & Abdullah, 2019),(b) (Naktong & Ruengwaree, 2020) and (c) (Arumugam et al., 2021)

4. Additional Effects of Decoupling Techniques

4.1. Analysis of External Decoupling

The external decoupling technique is the most widely utilized way for improving isolation. Although it has a great performance in decoupling, the comparisons in Tables 1, 2, 3, and 4 show more impacts and differences between various types of structures.

In Table 1 The NLs maintain a compact MIMO size that does not compromise the antenna substrate. Co-forming additional decoupling structures with antenna elements can improve antenna efficiency by improving insufficient matching

impedance. The low-profile metal lines do not raise the height of the MIMO system. Results from simulations show that adding decoupling lines reduces bandwidth.

To resist mutual coupling, the PDE shape is designed in a unique and flexible method. The impedance mismatch of antenna arrays can be fixed, and the impedance bandwidth increased by using extra metal patches. The decoupling structure blocks current flow, resulting in good gain for antenna elements loaded with parasitic patches as in Table 2. To provide a significant decoupling effect, parasitic patches are put indirectly above the substrate, increasing the height of the antenna systems.

Table 1. Comparison of literature review in Neutralization Line

Ref	Number of ports	Dimension (mm2)	Band width (GHz)	Isolation (dB)	Peak Gian (dBi)
[20]	4	48*34	3.5-10.08	23	Not mentioned
[21]	2	14.37*6.75	4.9-5.06	21.3	2
[22]	4	50*62	4.4–4.9	>20	2.5-3.1
[23]	2	46*46	3.1-11.7	16.5	Not mentioned
[24]	4	72*65	4.3-5.75	>20	3
[25]	2	56*48	2.2-2.42	46	Not mentioned
[26]	2	30*20	0.67-7.29	>18	3.37-6.2

Table 2. comparison of literature review in placing parasitic elements

Ref	Number of ports	Dimension (mm2)	Band width (GHz)	Isolation (dB)	Peak Gian(dBi)
[28]	2	45*30	2.5	15	2.65
[29]	2	40*23	3.2-17.8	20	4.93
[30]	2	55*33	2.1-18	45	6.5
[31]	2	40*50	4.3-7	28.5	6.5
[32]	2	23*45	5.9-6.1	33	-
[33]	2	114.5*94.9	3-6	13	7.96
[34]	2	14.76*8.38	28	35	6
[35]	4	28*28	38	32	7-9
[36]	4	54*54	3.1-11.8	20	6-35

In Table 3 Metamaterials can reduce coupling more effectively than other approaches due to their ability to control EM wave transmission. The metamaterial array also helps with gain enhancement. Some 3D structures are frequently used in metamaterials creation because they are complex and require more space to achieve the desired refractive indices, such as the popular mushroom form of EBG. To improve antenna performance in practical applications, Metamaterials are commonly paired with slots (Ali et al., 2018) or other structures to overcome challenges like as narrow bandwidth and high transmission power.

Table 3. comparison of literature review in Metamaterial

Ref	Number of ports	Dimension (mm2)	Band width (GHz)	Isolation (dB)	Peak Gian(dBi)	Metamaterial
[37]	2	30*30	2.6-12	20	5.5	EBG
[38]	4	30*40	3.1-6	16	3.5	EBG
[39]	2	31*26	3.1-11	>25	5.76	EBG
[40]	2	55.15*48	3.1-3.8	>20	Not mentioned	EBG
[41]	2	16*16	5.6-5.8 7.4-7.6 9.9-10.1	24.3	Not mentioned	EBG
[42]	4	48*48	3.3-3.7	25	Not mentioned	EBG
[43]	2	27*22	3.07-11.1	20	Not mentioned	EBG
[44]	2	30*60	3-12	23	9	EBG
[45]	2	35*50	3-11.1	24	9.6	
[46]	2	56*50	4-40	20	Not mentioned	EBG
[49]	2	18*9.2	28	30	7.8	SRR
[50]	2	48*35	2-18	27	8	SRR
[51]	4	70*70	2.5,3.3,3.5	28	1.74	SRR
[52]	4	40*40	2.4	>14	-	SRR
[53]	8	12*45.6	25-29.5	20	20.5	SRR
[55]	2	50*30	2.4,3.5	25,18	1.89	SRR
[54]	8	150*75	3.3-5	12	6	SRR
[56]	2	150*85	5.2	30	7	SRR

The DGS can be etched using simple methods and a low profile. It is possible to observe an improvement in efficient bandwidth as in Table 4. The inserted inductance slots will serve as resonator circuits at the working frequency, resulting

in a new resonance frequency. Furthermore, the background's DGS had no influence on the matching impedance. Furthermore, it has heat dissipation and is compatible with high power MIMO systems like mm-wave arrays. However, the radiation patterns have negative impacts on the DGS, causing it to emit undesired back radiation due to its defective structure. External decoupling offers advantages such as simple conception and efficiency in completion. The features of these decoupling strategies indicate that they are perfect for planar MIMO systems. However, high isolation of the antenna array was accomplished by modifying the shape and location of the decoupling structure. Currently, there is no systematic strategy to structural optimization, making external decoupling time-consuming.

Table 4. comparison of literature review in decoupling structure

Ref	Number of ports	Dimension (mm2)	Band width (GHz)	Isolation (dB)	Peak Gian(dBi)
[57]	2	26*40	2.2-11.4	20	2.4-7.5
[58]	2	30*18	4.3-15.63	20	2.5-5.35
[59]	2	20*29	5-13.5	21	5.5
[60]	2	20*31.5	3.25-3.85	19	5.9
[61]	4	72*72	2.8-13.3	18	Not mentioned
[62]	4	45*45	3.1-11	16	3.6
[63]	4	35.9*35.9	3.2-10.8	20	4.7
[64]	8	92*92	2.8-11	15	7.2
[65]	6	71*95	2.9-11	20	8
[66]	4	58*58	2.8-12.1	20	5.96

4.2. Analysis of Internal Decoupling

Internal decoupling strategies have lately become well-established. The research on internal decoupling focused on polarization diversity. To ensure that diverse signals correlated as little as possible, orthogonal modes were constructed. The performance of these self-decoupling MIMO systems is observed in Table 5.

Table 5. comparison of literature review in placing antenna elements in orthogonality

Ref	Number of ports	Dimension (mm2)	Band width (GHz)	Isolation (dB)	Peak Gian(dBi)
[67]	4	37*46	2.5-12	20	4
[68]	2	80*80	2.6-11	17.4	3.38
[69]	4	50*50	3-12	20	5.76
[70]	4	50*50	3.1-10.6	>17	4.84
[71]	4	92*92	2-14	15	7.2
[72]	4	48*48	3.2-11.2	20	Not mentioned
[73]	4	40*40	3.2-11.4	20	Not mentioned
[74]	4	52*52	1.25-40	18	4-4.5

Polarization diversity can lead to increased isolation within a common radiation element through internal decoupling. In addition to significant decoupling, polarization diversity can effectively prevent multipath effects and fading. Thus, these self-decoupling MIMO systems display excellent multi-directional robustness compared to single-polarized systems in some scattering propagation settings (Sousa De Sena et al., 2019), demonstrating their enormous potential to deploy in massive MIMO for large-scale wireless communication devices; While polarization improves isolation, it cannot reduce surface current. Simply choosing internal decoupling is insufficient for MIMO systems.

4.3. Future Direction Discussion

Although MIMO antenna isolation has been improved, designing decoupling systems with strong isolation and compact size remains a problem. Potential work areas include:

1. Hybrid decoupling structures

To mitigate coupling effects, many decoupling approaches have been developed. The decoupling methods listed above have different characteristics. Some are efficient at suppressing space waves, while others block surface waves. However, the mutual coupling effect is caused by interference from several sources of radiation elements, rather than one reason. Hybrid decoupling structures can be used to improve isolation by focusing on several interference paths.

2. Low Complexity

Complexity is a challenge to using decoupling approaches effectively. Coupling reduction schemes now require many branches or arrays of decoupling components to achieve excellent isolation and cover a wider bandwidth. However, adding more decoupling structures into MIMO systems increases device complexity. Choosing isolation over physical space is not recommended in the long term. Further developments may include the use of novel substrate materials. Mutual coupling is affected by substrate dielectric constant and thickness. Materials with low dielectric constants can help compensate for limitations in decoupling, in addition to traditional decoupling methods.

3. Systematic optimization procedure

In terms of ordinary coupling reduction strategies, most of these solutions depend heavily on engineers' previous experience. There are no generic optimization algorithms for the MIMO system for choosing the ideal decoupling point or adjusting the decoupling structure's parameters.

5. Conclusion

This review analyzes MIMO antennas for UWB, including mutual coupling approaches and performance comparisons. The paper highlights key issues for MIMO antenna designers, such as minimizing mutual coupling, obtaining compactness, covering diverse frequency bands, and improving overall performance. Future MIMO antennas should be designed to work easily with existing technologies, be compact and adaptable, and have real-time performance monitoring. This paper emphasizes the significance of evaluating MIMO antennas using different performance criteria, such as far-field and gain.

References

Abbas, A., Hussain, N., Sufian, M. A., Awan, W. A., Jung, J., Lee, S. M., & Kim, N. (2023). Highly selective multiple-notched UWB-MIMO antenna with low correlation using an innovative parasitic decoupling structure. *Engineering Science and Technology, an International Journal*, 43. https://doi.org/10.1016/j.jestch.2023.101440

Abbas, S. M., Desai, S. C., Esselle, K. P., Volakis, J. L., & Hashmi, R. M. (2018). Design and Characterization of a Flexible Wideband Antenna Using Polydimethylsiloxane Composite Substrate. *International Journal of Antennas and Propagation*, 2018. https://doi.org/10.1155/2018/4095765

Abbouda, A. A., El-Sallabi, H. M., & Haggman, S. G. (2006, July). Effect of mutual coupling on BER performance of Alamouti scheme. *IEEE Antennas and Propagation Society International Symposium*, 2006 (pp. 4797-4800). IEEE.

Addepalli, T., Desai, A., Elfergani, I., Anveshkumar, N., Kulkarni, J., Zebiri, C., Rodriguez, J., & Abd-Alhameed, R. (2021). 8-port semi-circular arc mimo antenna with an inverted l-strip loaded connected ground for uwb applications. *Electronics (Switzerland)*,10(12) https://doi.org/10.3390/electronics10121476

Alharbi, A. G., Rafique, U., Ullah, S., Khan, S., Abbas, S. M., Ali, E. M., Alibakhshikenari, M., & Dalarsson, M. (2022). Novel MIMO Antenna System for Ultra Wideband Applications. *Applied Sciences (Switzerland)*, 12(7). https://doi.org/10.3390/app12073684

Ali, T., Saadh Aw, M., & Biradar, R. C. (2018). A Compact Bandwidth Enhanced Antenna Loaded with SRR For WLAN/WiMAX/Satellite Applications. *ADVANCED ELECTROMAGNETICS* (Vol. 7, Issue 4).

Arumugam, S., Manoharan, S., Palaniswamy, S. K., & Kumar, S. (2021). Design and performance analysis of a compact quad-element uwb mimo antenna for automotive communications. *Electronics (Switzerland)*, 10(18). https://doi.org/10.3390/electronics10182184

Awan, W. A., Zaidi, A., Hussain, M., Hussain, N., & Syed, I. (2021). The design of a wideband antenna with notching characteristics for small devices using a genetic algorithm. *Mathematics*, *9*(17). https://doi.org/10.3390/math9172113

Babu, N. S., Ansari, A. Q., Kanaujia, B. K., Singh, G., & Kumar, S. (2023). A two-port UWB MIMO antenna with an EBG structure for WLAN/ISM applications. *Materials Today: Proceedings*, 74, 334–339. https://doi.org/10.1016/j.matpr.2022.08.316

Balanis, C. A. (1992). Antenna theory: A review . *Proc. IEEE*, 7–23.

Beverage, H. H., & Peterson, H. O. (1931). Diversity receiving system of RCA communications, inc., for radiotelegraphy. *Proceedings of the Institute of Radio Engineers*, 19(4), 529-561.

Bsrat, G. G., Aruna, S., & Naik, K. S. (2022). Quad-Element MIMO Antenna with Enhanced Isolation for UWB Applications. *ECS Transactions*, 107(1), 2819–2835. https://doi.org/10.1149/10701.2819ecst

Chen, X. ; Z. S. ; L. Q. (2018). A Review of Mutual Coupling in MIMO Systems. *IEEE Access*, 24706–24719.

Christina, A., Malathi, J., Vamsi, B., Reddy, K., & Phanindra, K. R. (2024). *A Decoupling method using Split Ring Resonator (SRR) for Tri-band MIMO Antenna for WLAN LTE Band and 5G applications* (Vol. 13, Issue 1).

Devana, V. N. K. R., Radha, N., Sunitha, P., Alsunaydih, F. N., Alsaleem, F., & Alhassoon, K. (2024). Compact MIMO UWB antenna integration with Ku band for advanced wireless communication applications. *Heliyon*, 10(5). https://doi.org/10.1016/j.heliyon.2024.e27393

Dkiouak, A., Ouahabi, M. El, Chakkor, S., Baghouri, M., Zakriti, A., & Lagmich, Y. (2023). High Performance UWB MIMO Antenna by Using Neutralization Line Technique. *Progress In Electromagnetics Research C* (Vol. 131).

Elabd, R. H., & Al-Gburi, A. J. A. (2023). SAR assessment of miniaturized wideband MIMO antenna structure for millimeter wave 5G smartphones. *Microelectronic Engineering*, 282. https://doi.org/10.1016/j.mee.2023.112098

Emam, A., El-Ghandour, O. M., Ouda, E. S., & Magdy, A. (2024). A Palms-Up Together Shape MIMO Antenna For Extended UWB Applications. *INTERNATIONAL JOURNAL OF MICROWAVE AND OPTICAL TECHNOLOGY*.

Esmail, B. A. F., Isleifson, D., & Koziel, S. (2024). Dual-band millimetre wave MIMO antenna with reduced mutual coupling based on optimized parasitic structure and ground modification. *Scientific Reports*, 14(1). https://doi.org/10.1038/s41598-024-71189-6

Foschini, G. J. ; G. M. J. (1998). On Limits of Wireless Communications in a Fading Environment when Using Multiple Antennas. *Wirel. Pers. Commun*, 311–335.

Godi, R. C., Patil, R. R., & Kinagi, R. S. (2024). Parasitic isolation structure for mutual coupling reduction in a multiple input multiple output antenna. *Bulletin of Electrical Engineering and Informatics*, 13(6), 4430–4438. https://doi.org/10.11591/eei.v13i6.7860

Govindan, T., Palaniswamy, S. K., Kanagasabai, M., & Kumar, S. (2022). Design and Analysis of UWB MIMO Antenna for Smart Fabric Communications. *International Journal of Antennas and Propagation*. https://doi.org/10.1155/2022/5307430

Huang, J., Shen, L., Xiao, S., Shi, X., & Liu, G. (2023). A Miniature Eight-Port Antenna Array Based on Split-Ring Resonators for 5G Sub-6 GHz Handset Applications. *Sensors*, 23(24). https://doi.org/10.3390/s23249734

Islam, T., Ali, E. M., Awan, W. A., Alzaidi, M. S., Alghamdi, T. A. H., & Alathbah, M. (2024). A parasitic patch loaded staircase shaped UWB MIMO antenna having notch band for WBAN applications. *Heliyon*, 10(1). https://doi.org/10.1016/j.heliyon.2023.e23711

J. Zhang, S. Y. X. H. G. A. E. V. (2020). Mutual coupling suppression for onbody multiantenna systems. *IEEE Trans Electromagn Compat*, 1045–1054.

Jabire, A. H., Ghaffar, A., Li, X. J., Abdu, A., Saminu, S., Alibakhshikenari, M., Falcone, F., & Limiti, E. (2021). Metamaterial based design of compact UWB/MIMO monopoles antenna with characteristic mode analysis. *Applied Sciences (Switzerland)*, 11(4), 1–21. https://doi.org/10.3390/app11041542

Janaswamy, R. (2002). Effect of element mutual coupling on the capacity of fixed length linear arrays. *IEEE Antennas Wirel. Propag. Lett*, 157–160.

Jayant, S., & Srivastava, G. (2023). Close-Packed Quad-Element Triple-Band-Notched UWB MIMO Antenna with Upgrading Capability. *IEEE Transactions on Antennas and Propagation*, 71(1), 353–360. https://doi.org/10.1109/TAP.2022.3222768

Jayant, S., Srivastava, G., & Kumar, S. (2022). Quad-Port UWB MIMO Footwear Antenna for Wearable Applications. *IEEE Transactions on Antennas and Propagation*, 70(9), 7905–7913. https://doi.org/10.1109/TAP.2022.3177481

Jensen, M. A. J. M. A. (2016). A history of MIMO wireless communications. *In Proceedings of the 2016 IEEE International Symposium on Antennas and Propagation (APSURSI),*.

Jetti, C. R., & Nandanavanam, V. R. (2018). Compact MIMO Antenna with WLAN Band-Notch Characteristics for Portable UWB Systems. *Progress In Electromagnetics Research C* (Vol. 88).

John, D. M., Vincent, S., Pathan, S., & Ali, T. (2024). Characteristics mode analysis based wideband Sub-6 GHz flexible MIMO antenna using a unique hybrid decoupling structure for wearable applications. *Physica Scripta*, 99(3). https://doi.org/10.1088/1402-4896/ad28a1

Kempanna, S. B., Biradar, R. C., Kumar, P., Kumar, P., Pathan, S., & Ali, T. (2023). Characteristic-Mode-Analysis-Based Compact Vase-Shaped Two-Element UWB MIMO Antenna Using a Unique DGS for Wireless Communication. *Journal of Sensor and Actuator Networks*, 12(3). https://doi.org/10.3390/jsan12030047

Khan, A., Bashir, S., Ghafoor, S., & Qureshi, K. K. (2021). Mutual Coupling Reduction Using Ground Stub and EBG in a Compact Wideband MIMO-Antenna. *IEEE Access*, *9*, 40972–40979. https://doi.org/10.1109/ACCESS.2021.3065441

Khan, A., He, Y., & Chen, Z. N. (2023). An Eight-Port Circularly Polarized Wideband MIMO Antenna Based on a Metamaterial-Inspired Element for 5G mmWave Applications. *IEEE Antennas and Wireless Propagation Letters*, 22(7), 1572–1576. https://doi.org/10.1109/LAWP.2023.3251740

Khan, D., Ahmad, A., & Choi, D. Y. (2024). Dual-band 5G MIMO antenna with enhanced coupling reduction using metamaterials. *Scientific Reports*, 14(1). https://doi.org/10.1038/s41598-023-50446-0

Khan, O., Khan, S., Marwat, S. N. K., Gohar, N., Bilal, M., & Dalarsson, M. (2023). A Novel Densely Packed 4 × 4 MIMO Antenna Design for UWB Wireless Applications. *Sensors (Basel, Switzerland)*, 23(21). https://doi.org/10.3390/s23218888

Khayat, M. A. ; W. J. T. ; J. D. R. ; L. S. A. (2000). Mutual coupling between reduced surface-wave microstrip antennas. *IEEE Trans. Antennas Propag*, 1581–1593.

Kulkarni, J., Desai, A., & Sim, C. Y. D. (2021). Wideband Four-Port MIMO antenna array with high isolation for future wireless systems. *AEU - International Journal of Electronics and Communications*, 128. https://doi.org/10.1016/j.aeue.2020.153507

Kumar, N., Kommuri, U. K., & Usha, P. (2023). Mutual Coupling Reduction in Multiband MIMO Antenna Using Cross-Slot Fractal Multiband EBG in the E-Plane. *Progress In Electromagnetics Research C* (Vol. 132).

Kumar, P., Pathan, S., Kumar, O. P., Vincent, S., Nanjappa, Y., Kumar, P., Shetty, P., & Ali, T. (2022). Design of a Six-Port Compact UWB MIMO Antenna with a Distinctive DGS for Improved Isolation. *IEEE Access*, 10, 112964–112974. https://doi.org/10.1109/ACCESS.2022.3216889

Kumar, S., Lee, G. H., Kim, D. H., Mohyuddin, W., Choi, H. C., & Kim, K. W. (2020). A compact four-port UWB MIMO antenna with connected ground and wide axial ratio bandwidth. *International Journal of Microwave and Wireless Technologies*, 12(1), 75–85. https://doi.org/10.1017/S1759078719000874

Kumar, S., Lee, G. H., Kim, D. H., Mohyuddin, W., Choi, H. C., & Kim, K. W. (2020). Multiple-input-multiple-output/diversity antenna with dual band-notched characteristics for ultra-wideband applications. *Microwave and Optical Technology Letters*, 62(1), 336–345. https://doi.org/10.1002/mop.32012

Lee, S. ; S. H. (2021). Accurate Statistical Model of Radiation Patterns in Analog Beamforming Including Random Error, Quantization Error, and Mutual Coupling. *IEEE Trans. Antennas Propag*, 3886–3896.

Li, W., Wu, L., Li, S., Cao, X., & Yang, B. (2024). Bandwidth Enhancement and Isolation Improvement in Compact UWB-MIMO Antenna Assisted by Characteristic Mode Analysis. *IEEE Access*, 12, 17152–17163. https://doi.org/10.1109/ACCESS.2024.3357629

Lim, E. G., Wang, Z., Lei, C. U., Wang, Y., & Man, K. L. (2010). Ultra wideband antennas: Past and present. *IAENG International journal of computer science*.

Ma, R., Huang, H., Li, X., & Wang, X. (2023). Triple-Band MIMO Antenna with Integrated Decoupling Technology. *International Journal of Antennas and Propagation* . https://doi.org/10.1155/2023/6691346

Masoodi, I. S., Ishteyaq, I., & Muzaffar, K. (2022). Extra Compact Two Element Sub 6 GHz MIMO Antenna for Future 5G Wireless Applications. *Progress In Electromagnetics Research Letters* (Vol. 102).

Mu, W., Lin, H., Wang, Z., Li, C., Yang, M., Nie, W., & Wu, J. (2022). A Flower-Shaped Miniaturized UWB-MIMO Antenna with High Isolation. *Electronics (Switzerland)*, 11(14). https://doi.org/10.3390/electronics11142190

Munusami, C., & Venkatesan, R. (2024). A Compact Boat Shaped Dual-Band MIMO Antenna With Enhanced Isolation for 5G/WLAN Application. *IEEE Access*, 12, 11631–11641. https://doi.org/10.1109/ACCESS.2024.3356078

Naktong, W., & Ruengwaree, A. (2020). Four-Port Rectangular Monopole Antenna for UWB-MIMO Applications. *Progress In Electromagnetics Research B* (Vol. 87).

Nikolic, M. M. ; D. A. R. ; N. A. (2005). Microstrip antennas with suppressed radiation in horizontal directions and reduced coupling. *IEEE Trans. Antennas Propag*, 3469–3476.

Nornikman, H., Ahmad, B. H., Aziz, M. A., Othman, A. R., & Malek, F. (2015). Split Ring Resonator Structure on Microstrip Patch Antenna and Other Microwave Application Design: A Review. *Journal of Telecommunication, Electronic and Computer Engineering (JTEC)*, *7*(2), 83-88.

Pandya, K., Upadhyaya, T., Patel, U., Sorathiya, V., Pandya, A., Al-Gburi, A. J. A., & Ismail, M. M. (2024). Performance analysis of quad-port UWB MIMO antenna system for Sub-6 GHz 5G, WLAN and X band communications. *Results in Engineering*, 22. https://doi.org/10.1016/j.rineng.2024.102318

Peterson, H. O., Beverage, H. H., & Moore, J. B. (1931). Diversity telephone receiving system of RCA Communications, Inc. *Proceedings of the Institute of Radio Engineers*, *19*(4), 562-584.

Pradeep, P., Basha, M. M., Gundala, S., & Syed, J. (2024). Development of Wearable Textile MIMO Antenna for Sub-6 GHz Band New Radio 5G Applications. *Micromachines*, *15*(5). https://doi.org/10.3390/mi15050651

Raheja, D. K., Kumar, S., & Kanaujia, B. K. (2020). Compact quasi-elliptical-self-complementary four-port super-wideband MIMO antenna with dual band elimination characteristics. *AEU - International Journal of Electronics and Communications*, *114*. https://doi.org/10.1016/j.aeue.2019.153001

Rajeshkumar, V., & Rajkumar, R. (2021). SRR Loaded Compact Tri-Band MIMO Antenna for WLAN/WiMAX Applications. *Progress In Electromagnetics Research Letters* (Vol. 95).

Sakli, H., Abdelhamid, C., Essid, C., & Sakli, N. (2021). Metamaterial-Based Antenna Performance Enhancement for MIMO System Applications. *IEEE Access*, *9*, 38546–38556. https://doi.org/10.1109/ACCESS.2021.3063630

Saxena, G., Prajapati, V., Gupta, V., & Kumar, S. (2021). High Isolation with Mushroom Shaped EBG Super Wide Band MIMO Antenna. *2021 International Conference on Advance Computing and Innovative Technologies in Engineering, ICACITE 2021*, 920–926. https://doi.org/10.1109/ICACITE51222.2021.9404651

Sengar, K. ; R. N. ; S. A. ; S. D. ; V. S. ; S. (2014). Study and Capacity Evaluation of SISO, MISO and MIMO RF Wireless Communication Systems. *Int. J. Eng. Trends Technol*, 436–440.

Sim, C. Y. D., Dhasarathan, V., Tran, T. K., Kulkarni, J., Garner, B. A., & Li, Y. (2023). Mutual Coupling Reduction in Dual-Band MIMO Antenna Using Parasitic Dollar-Shaped Structure for Modern Wireless Communication. *IEEE Access*, *11*, 5617–5628. https://doi.org/10.1109/ACCESS.2023.3235761

Singh, G., Kumar, S., Abrol, A., Kanaujia, B. K., Pandey, V. K., Marey, M., & Mostafa, H. (2023). Frequency Reconfigurable Quad-Element MIMO Antenna with Improved Isolation for 5G Systems. *Electronics (Switzerland)*, *12*(4). https://doi.org/10.3390/electronics12040796

Sousa De Sena, A., Benevides Da Costa, D., Ding, Z., & Nardelli, P. H. J. (2019). Massive MIMO-NOMA Networks With Multi-Polarized Antennas. *IEEE Transactions on Wireless Communications*, *18*(12), 5630–5642. https://doi.org/10.1109/TWC.2019.2937868

Srinubabu, M., & Venkata Rajasekhar, N. (2024). A compact and efficiently designed two-port MIMO antenna for N78/48 5G applications. *Heliyon*, *10*(7). https://doi.org/10.1016/j.heliyon.2024.e28981

Sultan, K. S., & Abdullah, H. H. (2019). Planar UWB MIMO-Diversity Antenna with Dual Notch Characteristics. In *Progress In Electromagnetics Research C* (Vol. 93).

Suresh, A. C., Reddy, T. S., Madhav, B. T. P., Das, S., Lavadiya, S., Algarni, A. D., & El-Shafai, W. (2022). Investigations on Stub-Based UWB-MIMO Antennas to Enhance Isolation Using Characteristic Mode Analysis. *Micromachines*, *13*(12). https://doi.org/10.3390/mi13122088

Suresh Babu, N., Quaiyum Ansari, A., Kumar Kanaujia, B., Singh, G., & Kumar, S. (2023). Compact two-port ultra-wideband multiple-input-multiple-output antenna with an electromagnetic band gap structure. *Materials Today: Proceedings*. https://doi.org/10.1016/j.matpr.2023.03.372

Tamminaina, G., & Manikonda, R. (2023). *Investigation on Performance of Four Port MIMO Antenna Using Electromagnetic Band Gap for 5G Communication* (Vol. 119).

Tan, X., Wang, W., Li, Y., Kishk, A. A., Tang, B., & Liu, Y. (2022). Isolation enhancement in planar multiple antenna by using split miniaturized-EBG structure. *International Journal of RF and Microwave Computer-Aided Engineering*, *32*(3). https://doi.org/10.1002/mmce.23027

Tiwari, R. N., Singh, P., Kanaujia, B. K., & Srivastava, K. (2019). Neutralization technique based two and four port high isolation MIMO antennas for UWB communication. *AEU - International Journal of Electronics and Communications*, *110*. https://doi.org/10.1016/j.aeue.2019.152828

Wallace, J. W. ; J. (2004). Mutual coupling in MIMO wireless systems: *A Rigorous Network Theory Analysis. IEEE Trans. Wirel. Commun.*, 1317–1325.

Wang, C. ; L. E. ; S. D. F. (2017). Surface-Wave Coupling and Antenna Properties in Two Dimensions. *IEEE Trans. Antennas Propag*, 5052–5060.

Wang, Z., Mu, W., Yang, M., & Li, C. (2022). Design of Compact Multiband MIMO Antenna Based on Ground Neutralization Line Decoupling. *Applied Computational Electromagnetics Society Journal*, *37*(6), 702–715. https://doi.org/10.13052/2022.ACES.J.370606

Weiss, A. J. ; F. B. (1988). Direction Finding in The Presence of Mutual Coupling. In Proceedings of the Twenty-Second Asilomar Conference on Signals, Systems and Computers. *Pacific Grove, CA*.

Zeain, M. Y., Abu, M., Althuwayb, A. A., Alsariera, H., Al-Gburi, A. J. A., Abdulbari, A. A., & Zakaria, Z. (2024). A New Technique of FSS-Based Novel Chair-Shaped Compact MIMO Antenna to Enhance the Gain for Sub-6GHz 5G Applications. *IEEE Access*, *12*, 49489–49507. https://doi.org/10.1109/ACCESS.2024.3380013

Zhao, X., Lee, Y., & Choi, J. (2011). Design of a compact patch antenna using split-ring resonator embedded substrate. *Microwave and Optical Technology Letters*, *53*(12), 2786–2790. https://doi.org/10.1002/mop.26411

Zou, X. J., Wang, G. M., Kang, G. Q., Song, W., Tan, M., Xu, X. G., & Zhu, H. (2023). Wideband coupling suppression with neutralization-line-incorporated decoupling network in MIMO arrays. *AEU - International Journal of Electronics and Communications*, *167*. https://doi.org/10.1016/j.aeue.2023.154688

How to Cite this Article:
Emam, A.A. *et al.* (2025) 'Analysis on Different Decoupling Methods for MIMO Antenna in Ultra-Wide Band Applications: A Review ', *Suez Canal Engineering, Energy and Environmental Science Journal*, 3(1), pp. 26-42